Multiuser - MIMO for Capacity Gain in Fi-Wi Hybrid Networks

D. Debbarma*, Q. Wang*, A. Lo#, S. M. Heemstra de Groot*, R. Venkatesha Prasad#, V. S. Rao#
Delft University of Technology
The Netherlands
{ A.C.C.Lo, R.R.VenkateshaPrasad, V.Rao } @tudelft.nl
* *Eindhoven University of Technology*
The Netherlands
{D.Debbarma, Qing.Wang, S.HeemstraDeGroot } @tue.nl

***Abstract*—*Fiber to the Rooms* paradigm is gaining a lot of attention recently. In this paradigm, the last mile wireless (*viz.*, IEEE 802.11x) connectivity, backed by optical fiber infrastructure, supports uncompressed high data rate while rendering seamless mobility and higher frequency reuse. To provide cost effective solution, Access Points (AP) in each room are replaced by distributed antennas. A centralized home communication controller provides AP functionality. WiFi inherently suffers from the problem of hidden nodes (HN). This problem persists even in the Fiber-Wireless (Fi-Wi) hybrid world causing degradation of throughput. In this paper we propose a Multi-User Multiple Input Multiple Output (MU-MIMO) uplink technique using both spatial and optical wavelength multiplexing. This scheme can increase the data rate significantly through diversity gain or spatial multiplexing. The proposed scheme is compared against an eminent joint decoding technique called Successive Interference Cancellation (SIC) adapted for operability in Fi-Wi indoor environment. The main contribution is that we propose an unique MU-MIMO uplink technique for Fi-Wi Hybrid indoor environment which address the problem of HN. We evaluate the performance of our proposed MU-MIMO technique based on ergodic capacity and probability of bit error.**

***Index Terms*—Fiber-Wireless, WiFi, Radio over Fiber, Successive Interference Cancellation, Multi-User Multiple input Multiple Output**

I. Introduction

Most of the broadband traffic in todays world can be accounted from indoor environments. For supporting such high rate applications in indoor environments, and to provide a future proof infrastructure installation, optical fibers are becoming very popular. Wireless coverage, on the other hand, offers the users with the much needed freedom of mobility. Thus hybrid Fi-Wi infrastructure is considered to be the future proof solution for broadband access in indoor environments [1], [2]. The Fi-Wi network described in our paper consists of a fiber infrastructure, controlled by a central Home Communication Controller (HCC). HCC serves as the brain of the network. Using Radio over Fiber (RoF) technology, the radio signals are distributed across the Cell Access Nodes (CANs) inside rooms to cover the immediate periphery of the indoor network (see Fig. 1). The CANs connected to the HCC form a Distributed Antenna System (DAS). DAS is energy efficient and can reduce the hardware cost of installation over longer period of time [3].

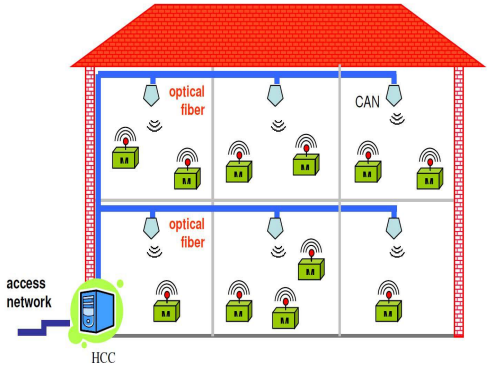

Fig. 1: Hybrid Fiber-Wireless Indoor Architecture

In this paper, we investigate the issue of improving the system capacity. The use of Fi-Wi channels provides the network with two degrees of freedom. Firstly, because of multiple optical wavelengths to carry the RF signals across different CANs. Next, the radio channels could be reused spatially at each CAN. Let us assume the underlying wireless standard to be IEEE 802.11x for Wireless LAN access indoor. For WiFi the medium access contention mechanism is CSMA/CA. If mobile terminals (MTs) across different CANs (operating at the same radio channel) are trying to access at the same time, a single WiFi Access Point (AP) located in the HCC[1], then we need to address the Hidden Nodes (HN) problem. These MTs at different CANs are deaf to each others ongoing transmission as they are outside each others sensing range. So when they transmit messages, these messages collide at the HCC as they are trying to access the same radio card irrespective of the way in which the messages are transported in the optical fiber. Hence none of the MTs are able to transmit their messages to HCC due to collision. This is usually referred in the literature as the HN problem. The HN problem in IEEE 802.11x has been extensively studied in [4], [5]. HN causes reduced throughput over the Fi-Wi channel. We can use RTS (Request to Send)/CTS (Clear to Send) mechanism to eliminate HNs, but this can adversely impact the performance

[1]Now on we use the term HCC to mean both HCC and the AP functionality at HCC.

of system by decreasing spatial reuse [6]. Moreover using the RTS/CTS mechanism makes sense only if the data packets length are larger than a threshold value. Hence it is not a generic solution for all size of data packets [7]. Even the use of Point Coordinated Function (PCF) at the HCC can help to solve the HN problem but it introduces more delay in the network as there is no simultaneous decoding for the MTs. Moreover hardly any APs available in todays world employ PCF.

We propose a special MU-MIMO uplink scheme taking advantage of both the spatial and optical multiplexing. We compare our proposed scheme against a legacy multiuser detection technique called SIC. SIC serves as a comparative benchmark criterion against the scheme proposed in this paper. The SIC receiver [8]implementation at the HCC makes it possible at the physical layer to decode messages from the MTs across different CANs, that arrive simultaneously. This yields better network capacity. The proposed MU-MIMO technique can be used to provide even larger network capacity gains for this sort of Fi-Wi scenario. A huge amount of literature is available about conventional MU-MIMO [9], [10], [11] techniques. Our proposed MU-MIMO scheme takes advantage of the spatially distributed MTs trying to talk with the MUMIMO-enabled CANs. Different optical wavelengths are used to transport the messages to the HCC where the decoding is done. The optical fiber provides huge bandwidth and is less error prone. In this work we assume that the error at the optical fiber part is negligible and thus we do not consider it for our analysis. We model and compare three cases of the network operation. In the first case, we choose independent transmissions where collisions are allowed as there is no successive decoding technique employed at the HCC. In the second case packet capture using SIC receiver at the HCC is considered. Finally both of them are compared to our proposed opto-spatial MU-MIMO uplink scheme.

This paper is organized as follow. Section II describes briefly the Fi-Wi system architecture. Section III provides an overview of SIC reception. We then analytically try to find the capacity that is achievable by using SIC receiver and compare it against the independent transmissions case where packet capture is not allowed at the HCC. Section IV explains the proposed MU-MIMO system architecture for Fi-Wi network and the capacity achievable. Section V tries to compare the network performance. Probability of bit-error is computed to give an idea of how good the system performs. Section VI presents the simulation results and finally we conclude in Section VII highlighting the achievements and throwing some light on the future outlook. beginfigure

II. System Architecture

Our approach is to design a managed hybrid Fi-Wi indoor network, consisting of fiber to the room and a last mile wireless infrastructure. It is a centralized architecture controlled by HCC. RoF is used to distribute radio signals throughout the building using CANs which acts as distributed antenna elements. The red lines in Fig. 2 represents the optical fibers.

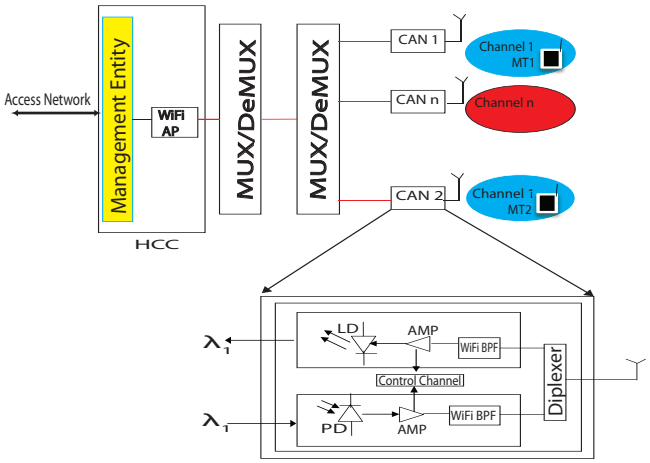

Fig. 2: Overall System architecture with the structure of CAN.

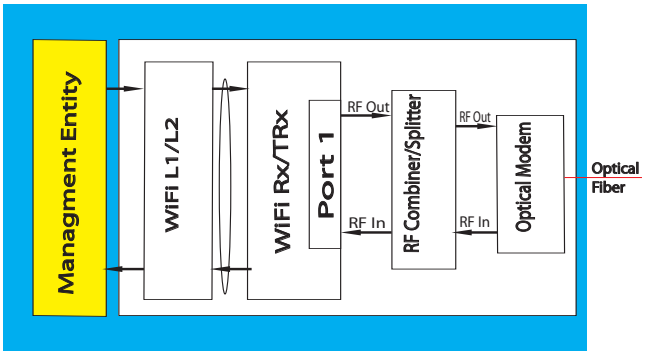

Fig. 3: Detailed structure of the HCC.

The CANs inside the rooms cover the immediate periphery. There is a single CAN per room or living space. Each radio cell is confined to the room or living space where WiFi is supported. We assume that there is no overlap between the radio cells. In Fig. 2, CAN 1 and CAN 2 are operating at the same radio channel as represented by the same color. The system architecture described in this section is applicable for the cases of independent transmissions and SIC as described in Section I. For MU-MIMO, the system architecture is a bit different and is explained later in Section IV.

The HCC essentially provides management functions. The optical modem inside HCC as shown in Fig. 3 modulates the RF signals in the downlink to tunable optical signals of different wavelength. The optical signals are then fed to MUX (multiplexer)/DeMUX (de-multiplexer) to guide them to CANs operating on particular wavelengths. The CANs employ simple optical to radio signal conversion using Photo-Diodes (PD). After amplification by amplifiers (AMP) the signals are fed to the wireless indoor environment using single element antennas. WiFi Band-pass filters (WiFi BPF) are employed to filter only the WiFi signals. In the uplink scenario, the same set of operations takes place but in the reverse order using different Laser Diodes (LD), AMPs and WiFi BPFs across different CANs. The laser sources used at the CANs are different and hence the nature of the Laser Diodes (LDs) are incoherent. When these LDs are used to modulate radio signals

onto optical wavelengths, the wavelengths do not clash even if same wavelength is used across those CANs to transport the MTs message. Hence satisfying the wavelength clash constraint for Wavelength Division Multiplexing (WDM). HCC hosts a single WiFi AP supporting multiple CANs in multiple rooms. Many CANs use the same frequency radio channels as there are only three non-overlapping channels available. The number of CANs are assumed to be more than the number of non-overlapping channels. In the later part, for analysis, we consider two such CANs operating at the same radio channel in different rooms trying to communicate with the HCC.

III. Successive Interference Cancellation (SIC)

A legacy technique in cellular networks for decoding messages that arrive simultaneously is SIC. It is the ability of the receiver to receive and decode two or more messages concurrently, which otherwise would have been lost due to collision. Recent advances in software defined radio like GNU radios [12], [13] has opened possibilities for SIC implementation in indoor. SIC receivers has been shown to be practically implementable in [12] for Zigbee (which operates in the same ISM band as that of WiFi) using software radios for wireless environment. With SIC, the message from MT with higher Received Signal Strength (RSS) is decoded first and then the reconstructed signal of that message is subtracted from the mixed signal to decode the weaker signal. The use of SIC receiver at the HCC helps to deal with the problem of HN. We defer from going into the implementation part of SIC receiver and focus on the physical layer aspects for our architecture. As mentioned earlier, SIC will serve as a comparative scheme to evaluate the performance of our proposed MU-MIMO scheme described later in Section IV. We assume that the MTs from different cells implementing SIC operate with different RSS. The assumption holds because of the heterogeneous nature of the rooms in which the MTs are operating. This leads to different channel gains which contributes to different RSS. We recognize that this assumption may not be ideal for WiFi indoor but never the less it is interesting to see how SIC performs over Fi-Wi indoor for WiFi.

A. System Model

We assume that two MTs are trying to communicate with HCC via two different CANs which are placed in two very different indoor locations. The cell area of the CANs does not overlap. The CANs are operating at the same radio frequency channel. The two MTs within those CANs trying to communicate with the HCC thus meet with collision if they try to send messages at the same time. By implementing SIC receiver at the HCC we can perform successive message decoding and thus increase spectral efficiency.

Let s_1 and s_2 be two messages that are being transmitted from two independent MTs. The receiver at the HCC receives,

$$y = \alpha_1 y_1 + \alpha_2 y_2, \tag{1}$$

where,

$$y_i = \sqrt{P_i} h_{ij} s_i + n_i, \tag{2}$$

where h_{ij} represents the respective channel gain from MT i to antenna j of CAN j. s_i is the message transmitted from MT i and n_i represents the noise. $P_i$represents the transmission power at MT i. Thus, (1) can be rewritten as,

$$\begin{aligned} y &= \alpha_1 y_1 + \alpha_2 y_2 \\ &= \alpha_1\sqrt{P_1}h_{11}s_1 + \alpha_2\sqrt{P_2}h_{22}s_2 + \underbrace{\alpha_1 n_1 + \alpha_2 n_2}_{n_0} \\ &= \alpha_1\sqrt{P_1}h_{11}s_1 + \alpha_2\sqrt{P_2}h_{22}s_2 + n_0, \end{aligned} \tag{3}$$

where $n_0 = \sqrt{N_0}$ and α's are the amplification factors and are calculated as follow,

$$P = \alpha_i^2 E[y_i]^2. \tag{4}$$

P represents the maximum power available at the CANs to amplify the messages received and send it over the optical fiber to the HCC. $E[\cdot]$ represents the expectation. Let B be the bandwidth of the operating wireless channel for CANs. The decodability of the two messages with SIC depends on the RSS and the transmission bit rates. When the two MTs as shown in Fig. 2 as MT 1 and MT 2 are transmitting concurrently to the HCC, HCC must decode the message with the stronger RSS first (without loss of generality, let us assume it to be s_1) treating the other one (i.e., s_2 in our case) as interference. Thus the rate achieved by MT 1 is,

$$\begin{aligned} r_1 &= B\log_2\left(1 + \frac{P_1|h_{11}|^2|\alpha_1|^2|s_1|^2}{P_2|h_{22}|^2|\alpha_2|^2|s_2|^2 + N_0}\right) \\ &= B\log_2\left(1 + \frac{S_1}{S_2 + N_0}\right), \end{aligned} \tag{5}$$

where, $N_0 = |\alpha_1 n_1 + \alpha_2 n_2|^2$ represents the noise variance and S_1, S_2 represents the RSS of the different MTs at the HCC after optical to radio conversion. Only if MT 1 transmits at rate r_1 or below, it can be decoded successfully by HCC. After that, HCC can attempt to decode MT 2's signal. The best feasible bit rate r_2 for MT 2 assuming perfect cancellation of MT 1's message is,

$$r_2 = B\log_2\left(1 + \frac{S_2}{N_0}\right). \tag{6}$$

It is interesting to note that to facilitate SIC, MT 1 with stronger RSS may achieve rate lower than the weaker RSS achievable by MT 2. This is due to the fact that MT 1 decode in presence of noise and interference from MT 2 but MT 2 decodes just in the presence of noise.

B. Capacity without and with SIC

Let us now compare the capacity of Fi-Wi channel without and with SIC.

1) Without SIC: Without SIC only one of MT 1 and MT 2 can transmit at a time as there is no packet capture technique applied at the physical layer. If they transmit together then the transmission collides at the HCC. Let us assume that the collision probability at the HCC for the messages transmitted from MTs at different CANs be τ . So the capacity of the channel is given by,

$$\begin{aligned} C_{\text{withoutSIC}} = \max\Bigg\{&(1-\tau)B\log_2\left(1 + \frac{S_1}{|\alpha_1 n_1|^2}\right), \\ &(1-\tau)B\log_2\left(1 + \frac{S_2}{|\alpha_2 n_2|^2}\right)\Bigg\} \end{aligned} \tag{7}$$

2) With SIC: It is possible to simultaneously receive two messages. The highest bit rates at which MT 1 and MT 2 can successfully transmit concurrently are r_1 and r_2 respectively assuming perfect rate adaptation. Corresponding hybrid Fi-Wi channel capacity with SIC can be given by [13],

$$\begin{aligned} C_{\text{withSIC}} &= B\log_2\left(1+\frac{S_1}{S_2+N_0}\right)+B\log_2\left(1+\frac{S_2}{N_0}\right) \\ &= B\log_2\left(1+\frac{S_1+S_2}{N_0}\right). \end{aligned} \tag{8}$$

We assume that the channel varies with time. Thus, the capacity gain with SIC for the Fi-Wi environment is said to be the gain in ergodic capacity that we achieve using SIC over the case when we do not implement SIC and is given by,

$$\begin{aligned} \varpi &= \frac{E[C_{\text{withSIC}}]}{E[C_{\text{withoutSIC}}]}, \\ &= \frac{E\left[B\log_2\left(1+\frac{S_1+S_2}{N_0}\right)\right]}{E\left[(1-\tau)B\log_2\left(1+\frac{S_1}{|\alpha_1 n_1|^2}\right)\right]} \end{aligned} \tag{9}$$

The maximum capacity gain is attained at the point where both of $S_1 > S_2$ and $S_2 > S_1$ cases attain same capacity gains. Thus equating both the cases we attain the respective RSS at which maximum of relative capacity gain is achieved and is given below as,

$$\frac{E\left[B\log_2\left(1+\frac{S_1+S_2}{N_0}\right)\right]}{E\left[(1-\tau)B\log_2\left(1+\frac{S_1}{|\alpha_1 n_1|^2}\right)\right]} = \frac{E\left[B\log_2\left(1+\frac{S_1+S_2}{N_0}\right)\right]}{E\left[(1-\tau)B\log_2\left(1+\frac{S_2}{|\alpha_2 n_2|^2}\right)\right]} \tag{10}$$

Thus for maximizing the relative capacity gain we need to operate at RSS's given by,

$$S_1 = S_2\left(\frac{|\alpha_1 n_1|^2}{|\alpha_2 n_2|^2}\right). \tag{11}$$

We assume that full channel state information (CSI) is available at HCC. HCC can compute the optimal power levels for MTs as shown by (11). It can map the optimal power levels to a code word from a specific codebook. The codebook can be assumed to be known apriori to both HCC and the MTs. HCC can feedback the code word information to the MTs involved. Thus MTs can control their transmission power changing their modulation or coding schemes using that code word information. We refer to this as transmission power control scheme with SIC. This in fact makes implementation of SIC indoor realizable. We can always make sure that the RSSs of the MTs are very different due to transmit power control.

The average transmission time needed to send the messages from MTs to HCC with and without SIC can be given as,

$$\begin{aligned} \lambda_{\text{withoutSIC}} &= \frac{L}{E\left[(1-\tau)B\log_2\left(1+\frac{S_1}{|\alpha_1 n_1|^2}\right)\right]}+ \\ &\quad \frac{L}{E\left[(1-\tau)B\log_2\left(1+\frac{S_2}{|\alpha_2 n_2|^2}\right)\right]} \end{aligned} \tag{12}$$

$$\begin{aligned} \lambda_{\text{withSIC}} &= \max\left\{\frac{L}{E\left[B\log_2\left(1+\frac{S_2}{N_0}\right)\right]},\right. \\ &\quad \left.\frac{L}{E\left[B\log_2\left(1+\frac{S_1}{S_2+N_0}\right)\right]}\right\}. \end{aligned} \tag{13}$$

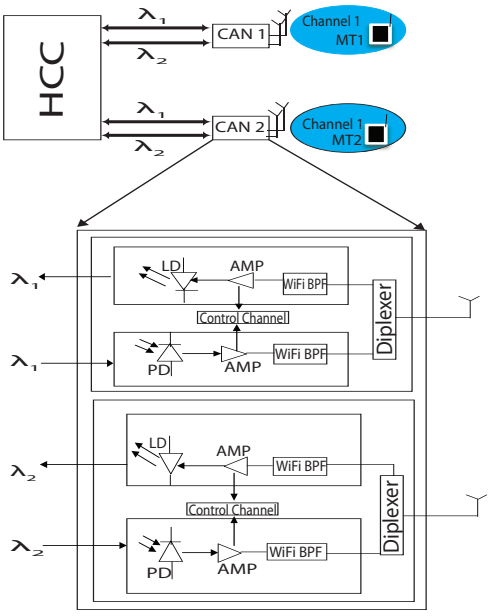

Fig. 4: CAN supporting multiuser-MIMO.

L represents the average packet length. The transmission rates for the two MTs transmissions with SIC from the MTs are different. So we are faced with a problem of disparity in rates which leads to inequality in transmission time. We can have equal average transmission time with SIC for both MTs. This will improve the MAC throughput as suggested in [13]. Interesting fact to note is that, there is a fine balance between increasing MAC throughput and physical layer capacity. We can either be greedy and choose to maximize the systems ergodic capacity, or we can provide equal average transmission time to both the MTs and be fair. If MTs have global CSI knowledge, then they can vary their transmission powers as below,

$$P_1 \approx \frac{P|h_{22}|^4 E[y_1]^2 P_2^2}{|h_{11}|^2 E[y_2]^4}. \tag{14}$$

Thus (14) helps to achieve maximum MAC throughput. This is possible as HCC acts as a centralized system. It has full CSI which it can share with the MTs.

IV. Multi User-Multiple Input Multiple Output (MU-MIMO)

Our proposed MU-MIMO architecture makes use of the idea of optical-spatial multiplexing to maximize ergodic capacity. MU-MIMO technology exploits the availability of multiple independent MTs in order to enhance the communication capabilities of each individual MTs. To the best of our knowledge this is the first work in Fi-Wi domain that explains a unique uplink optical-spatial multiplexing scheme.

A. System Architecture

To give a brief idea about our MU-MIMO scheme let us look at Fig. 4 and Fig. 5. If we consider the uplink, MT i at CAN i gets two different views of the channel as there are two antennas at each CAN and will be sending say message s_i . In the fiber part we use two different wavelengths (*eg.* λ_1, λ_2) per CAN. They carry the messages from different antennas across the same CAN to the HCC. At the HCC

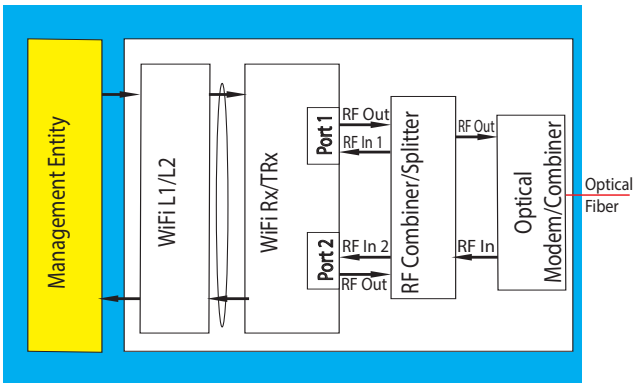

Fig. 5: HCC with Multiuser MIMO.

the message set (s_1, s_2) of the same wavelength are mixed together in optical domain and are converted back to radio signals using an optical modem/combiner, which are fed into the WiFi transceiver (Rx/TRx) at different ports. Thus, we are able to combine multiple messages from MTs across different antennas in CANs to take advantage of MIMO. This proposed scheme takes advantage of the optical wavelength multiplexing for the spatial multiplexed signals from the different CANs to attain MU-MIMO capabilities.

B. System Model

The receiver located in HCC receives two inputs which can be written into matrix form as,

$$\bar{y} = H\bar{s} + \bar{n} \tag{15}$$

where, $H = \begin{bmatrix} \alpha_1 h_{11'} & \alpha_2 h_{21} \\ \alpha_1 h_{12'} & \alpha_2 h_{22} \end{bmatrix}$, represents the amplified channel gain matrix, h_{ij} represents the channel gain from MT i to antenna j of the CAN under consideration. $j\epsilon(1', 2')$ represents the antennas across CAN 1 and similarly $j\epsilon(1, 2)$ represents the antennas across CAN 2. $\bar{s} = \begin{bmatrix} \sqrt{P_1}s_1 \\ \sqrt{P_2}s_2 \end{bmatrix}$ represents the messages transmitted. and $\bar{n} = \begin{bmatrix} N_1 \\ N_2 \end{bmatrix}$ represents the noise vector at the HCC where $N_1 = (\alpha_1 n_{1'} + \alpha_2 n_1)$, $N_2 = (\alpha_1 n_{2'} + \alpha_2 n_2)$. (n_1, n_2) represents the noise added at CAN 2 and similarly $(n_{1'}, n_{2'})$ represents the noise added at CAN 1 across the two different antennas at the CANs.

The value of the amplification factors α_1 and α_2 can be computed from the equations as follows,

$$\begin{aligned} {\alpha_1}^2|h_{11'}|^2 P_1 + {\alpha_1}^2|n_{1'}|^2 + \\ {\alpha_1}^2|h_{12'}|^2 P_1 + {\alpha_1}^2|n_{2'}|^2 = P \end{aligned} \tag{16}$$

$$\begin{aligned} {\alpha_2}^2|h_{21}|^2 P_2 + {\alpha_2}^2|n_1|^2 + \\ {\alpha_2}^2|h_{22}|^2 P_2 + {\alpha_2}^2|n_2|^2 = P \end{aligned} \tag{17}$$

P represents the total power available at the individual CANs to amplify the signals received. We assumed that the variance of messages to be 1. Therefore,

$${\alpha_1}^2 = \frac{P}{E[x_{1'}]^2 + E[x_{2'}]^2} \tag{18}$$

$${\alpha_2}^2 = \frac{P}{E[x_1]^2 + E[x_2]^2} \tag{19}$$

where $E[x_{1'}]^2 = |h_{11'}|^2 P_1 + |n_{1'}|^2$ and similarly others. The expression for capacity is given by,

$$C_{\text{MU-MIMO}} = E_H\left[B\log_2\|I + (H)K_s(H)^H Cov^{-1}\|\right] \tag{20}$$

where, K_s is the signal variance matrix assuming independent messages and Cov is covariance matrix of the noise, I refers to the identity matrix and $\|\cdot\|$ represents the determinant.The message transmission time for MU-MIMO case can thus be given by,

$$\lambda_{\text{MU-MIMO}} = \frac{2L}{C_{\text{MU-MIMO}}} \tag{21}$$

The capacity gain that we get with MU-MIMO in comparison with SIC and without SIC implementation can thus be given by,

$$\zeta = \frac{C_{\text{MU-MIMO}}}{E[C_{\text{withSIC}}]} \tag{22}$$

$$\delta = \frac{C_{\text{MU-MIMO}}}{E[C_{\text{withoutSIC}}]} \tag{23}$$

V. Probability of Bit Error

Probability of bit error [14] serves as a basic parameter in judging the performance of a system. It represents the probability that the bit transmitted is in error due to the noise and interference introduced by the channel. We now calculate the probability of bit error for various cases.

A. Without SIC

The bit error probability is the expectation over the value of bit error rate. IEEE $802.11b/n$ operating at 1 Mbps rate is a DSSS-DBPSK (Direct sequence spread spectrum-Differential Binary Phase Shift Keying) system. In order to obtain the bit error probability in a Rayleigh fading channel [15], [16] we first obtain its instantaneous SNR (Signal to nose ratio), γ_i as,

$$\gamma_i = h_{ii}^2 \frac{E_{b_i}}{|n_i|^2} \tag{24}$$

h_{ii} represents the channel gain from MT i to CAN i which is a Rayleigh distributed random variable, E_{b_i} represents the bit energy across MT i and n_i represents the noise at CAN i. Average SNR for Rayleigh faded channel at CAN i can thus be computed as,

$$\bar{\gamma_i} = E[h_{ii}]^2 \frac{E_{b_i}}{|n_i|^2} = 2\sigma^2 \frac{E_{b_i}}{N_0} \tag{25}$$

where, $2\sigma^2$ represents the variance of the channel. The probability distribution function of the Rayleigh distribution can be given as [14],

$$P^{(\text{Rayleigh})}(h_{ii}) = \begin{cases} \frac{h_{ii}}{\sigma^2} exp\left(-\frac{h_{ii}^2}{2\sigma^2}\right) & \text{if } 0 \leq h_{ii} \leq \infty \\ 0 & \text{if } h_{ii} < 0 \end{cases}$$

Thus $P^{(\text{Rayleigh})}(h_{ii})$ can be expressed with respect to instantaneous SNR, γ_i as,

$$\begin{aligned} P^{(\text{Rayleigh})}(\gamma_i) &= \frac{P^{(\text{Rayleigh})}(h_{ii})}{|\frac{d\gamma_i}{dh_{ii}}|} \\ &= \frac{1}{\bar{\gamma_i}} exp\left(-\frac{\gamma_i}{\bar{\gamma_i}}\right) \quad 0 \leq \gamma_i \leq \infty \end{aligned} \tag{26}$$

Therefore, probability of bit error for a single MT's transmission, as shown in [15], can be given as,

$$P_{\text{BER}}^{(\text{DBPSK-Rayleigh})} = \int_0^\infty \frac{1}{2} exp(-\gamma_i) \frac{1}{\bar{\gamma_i}} exp(-\frac{\gamma_i}{\bar{\gamma_i}}) d\gamma_i. \tag{27}$$

Probability of bit error, as shown in [15], for MT i can thus found out to be,

$$P_{\text{BER}}^{\text{(DBPSK-Rayleigh)}} = \frac{1}{2(1+\bar{\gamma_i})}. \quad (28)$$

Therefore bit error rate without SIC for both MTs is thus the summation of the bit error rate from MT 1 and MT 2 and can be given by,

$$P_{\text{BER}}^{\text{(withoutSIC)}} = \frac{1}{2(1+\bar{\gamma_1})} + \frac{1}{2(1+\bar{\gamma_2})}. \quad (29)$$

B. With SIC

With SIC, decoding is done successively in the presence of interference from other messages. Thus the instantaneous SNR for the first message can be given as,

$$\gamma_1 = \frac{\alpha_1^2 h_{11}^2 E_{b_1}}{\alpha_2^2 h_{22}^2 E_{b_2} + N_0}. \quad (30)$$

$N_0 = |\alpha_1 n_1 + \alpha_2 n_2|^2$ represents the noise variance at HCC. After decoding the first message, the second message can be decoded after subtracting the first message's signal from the mixed signal combination. The instantaneous SNR of the second message can be written as,

$$\gamma_2 = \frac{\alpha_2^2 h_{22}^2 E_{b_2}}{N_0}. \quad (31)$$

The average signal to interference noise ratio can be given by taking expectation over (30), (31) as, small

$$\bar{\gamma_1} = \frac{\alpha_1^2 2\sigma^2 E_{b_1}}{\alpha_2^2 2\sigma^2 E_{b_2} + N_0} \quad (32)$$

$$\bar{\gamma_2} = \frac{\alpha_2^2 2\sigma^2 E_{b_2}}{N_0}, \quad (33)$$

where we assume that the variance of both channels are the same i.e., $E[h_{11}^2] = E[h_{22}^2] = 2\sigma^2$. Thus $P^{\text{(Rayleigh)}}(h_{11})$ can be expressed with respect to instantaneous SNR, γ_1 as,

$$P^{\text{(Rayleigh)}}(\gamma_1) = \frac{P^{\text{(Rayleigh)}}(h_{11})}{|\frac{d\gamma_1}{dh_{11}}|} = \frac{a}{b\bar{\gamma_1}} exp\left(-\frac{\gamma_1 a}{\bar{\gamma_1} b}\right) \; 0 \leq \gamma_1 \leq \infty, \quad (34)$$

where $a = \alpha_2^2 h_{22}^2 E_{b_2} + N_0$ and $b = \alpha_2^2 E[h_{22}^2] E_{b_2} + N_0$ Thus probability of bit error, for MT 1 is,

$$P_{\text{BER-MT 1}}^{\text{(DBPSK-Rayleigh)}}(\text{withSIC}) = \frac{a}{2(a+b\bar{\gamma_1})} \quad (35)$$

Similarly for MT 2 the $P^{\text{(Rayleigh)}}(h_{22})$ can be expressed with respect to instantaneous SNR γ_2 as

$$P^{\text{(Rayleigh)}}(\gamma_2) = \frac{P^{\text{(Rayleigh)}}(h_{22})}{|\frac{d\gamma_2}{dh_{22}}|} = \frac{1}{\bar{\gamma_2}} exp\left(-\frac{\gamma_2}{\bar{\gamma_2}}\right) \; 0 \leq \gamma_2 \leq \infty \quad (36)$$

Thus probability of bit error for MT 2 would be,

$$P_{\text{BER-MT 2}}^{\text{(DBPSK-Rayleigh)}}(\text{withSIC}) = \frac{1}{2(1+\bar{\gamma_2})} \quad (37)$$

Thus the probability of bit error can be given by,

$$P_{\text{BER}}^{\text{(withSIC)}} = \max\left(\frac{a}{2(a+b\bar{\gamma_1})}, \frac{1}{2(1+\bar{\gamma_2})}\right) \quad (38)$$

C. MU-MIMO

For finding the probability of bit error for our special MU-MIMO uplink scheme we need to know how the decoding is done. The simplest of the decoder being Zero-Forcing (ZF) decoder, we use it for our analysis. We have two MTs namely MT 1 and MT 2 and two receiving ports in HCC. The channel matrix is represented as,

$$\mathbf{H} = \left[\; \mathbf{h}_1, \mathbf{h}_2 \; \right]^T \quad (39)$$

where $h_1 = (h_{11'}, h_{12'})$ and $h_2 = (h_{21}, h_{22})$, $[\sim]^T$ represents the transpose of the matrix and h_{ij} are Rayleigh with mean 0 and variance $2\sigma^2$. We assume for simplicity that the amplification factors are all set to unity. The post detection SNR of the i^{th} MT after ZF decoding, as given in [10] is,

$$\gamma_i = \frac{\gamma_0}{[(H^h H)^{-1}]_{ii}} \quad (40)$$

where H^h represents the Hermitian of the matrix H and γ_0 is the transmitted SNR for each antenna pair. We look closely at the distribution of $\frac{1}{[(H^h H)^{-1}]_{ii}}$ which is a Gamma distribution with two degrees of freedom and variance σ^2 .

Consequently the post detection SNR of the MT i has a pdf as,

$$f_2(\gamma_i) = \frac{1}{2\sigma^2\gamma_0} exp\left(-\frac{\gamma_i}{2\sigma^2\gamma_0}\right) \quad (41)$$

Thus to find the average bit error rate we have to find $P[\gamma_i \leq \gamma_{th}]$. Thus we first find the CDF of the post detection SNR.

$$P[\gamma_i \leq \gamma_{th}] = \int_0^{\gamma_{th}} \frac{1}{2\sigma^2\gamma_0} exp\left(-\frac{\gamma_i}{2\sigma^2\gamma_0}\right) d\gamma_i \quad (42)$$

THe BER of MU-MIMO which is the CDF can be given as,

$$P_{\text{BER}}^{\text{(MU-MIMO)}} = P[\gamma_i \leq \gamma_{th}] = 1 - exp\left(-\frac{\gamma_{th}}{2\sigma^2\gamma_0}\right). \quad (43)$$

The value of γ_{th} can be set from the knowledge of channel states. For our above analysis we choose to take the same threshold for both the MTs. The above equation (43) is true because the system decodes both the messages at the same time. Hence the system has the probability of bit error which is the maximum of the two MTs probability of error.As we set the parameters to be the same, so it turns out to be equal to the single MTs probability of bit error.

VI. Results and Discussion

In the mathematical analysis from previous sections we assumed that two MTs are trying to communicate to the HCC via two different CANs which are placed in two very different indoor locations. The cell area of the CANs does not overlap. The CANs are operating at the same radio frequency channel. The messages from different CANs are carried by same wavelength set (λ_1, λ_2) per CAN for MUMIMO case and same wavelength λ_1 in SIC and independent transmission case. The results from the mathematical analysis are used to generate the graphs in Matlab. We run Monte Carlo simulations for 20000 iterations to generate the plots. The wireless channels generated for simulations are assumed to be Rayleigh faded with mean 0 and variance 1. The probability of collision for non-SIC case is kept at 0.34. We recognize that it is quite high.

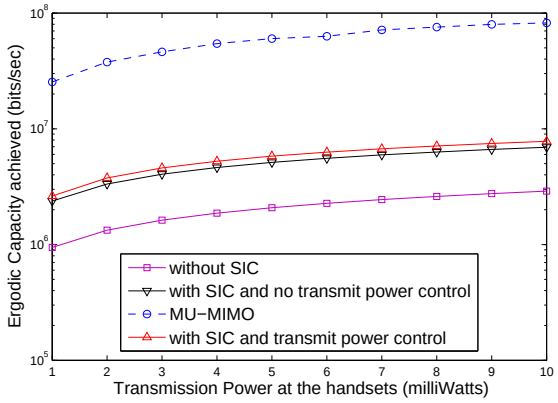

Fig. 6: Capacity of different schemes vs. Transmission power at the MTs.

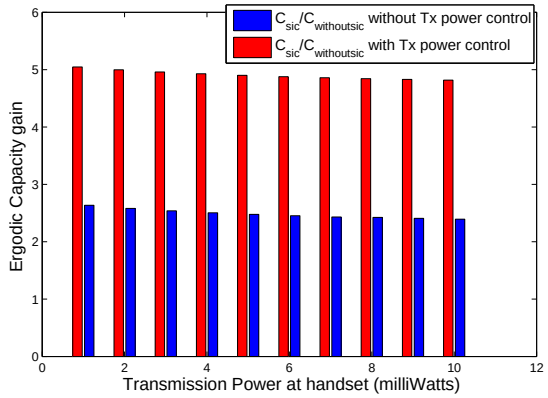

Fig. 7: Ergodic Capacity gain with and without SIC vs. Transmission Power at MTs.

However to study the scenario of higher traffic we selected this. We have set this in an arbitrary fashion. However the analysis holds good for any value of probability of collision. Fig. 6 compares the ergodic capacity achieved by different transmission schemes against the transmission power at the MTs. In this plot the power across both the MTs are kept the same, and are varied from $1-10\,\mathrm{mW}$.

In our analysis and simulation, we assumed that the optical channel is ideal. The inclusion of a more realistic optical channel model with independent gains is beyond the purview

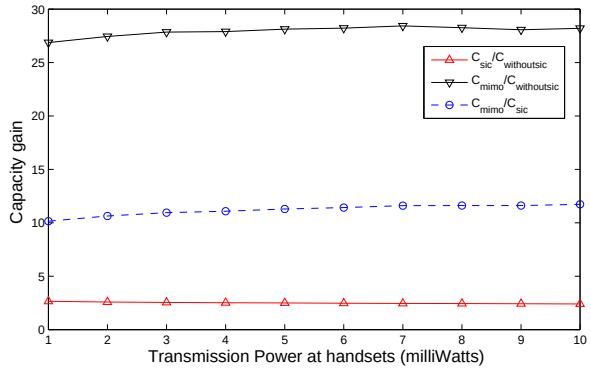

Fig. 8: Capacity gain vs. the Transmission Power at MTs.

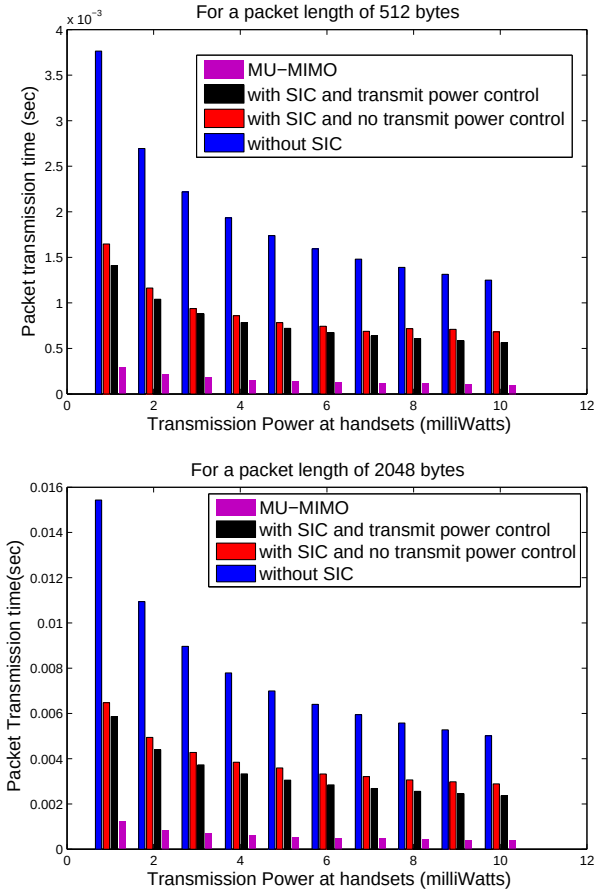

Fig. 9: Packet transmission time vs. Transmission Power for different packet lengths(512 bytes, 2048 bytes).

of this work (it is indeed the next step of our analysis). ThE underlying study in this paper serves as a basis for further study. We assume that we have full CSI at the HCC. The way the transmit power control is done at the HCC is given by (11) where the RSS's from the MTs are controlled such that maximum capacity gain is achieved for SIC. In Fig. 7 the ergodic capacity gains are plotted for SIC and non SIC case with and without power control at different values of transmit power at MT 1. The capacity gain achieved for SIC with and without transmit power control are more than double the capacity of without SIC. This is true because of the assumption of perfect rate adaptation and high probability of collision for non SIC case. Fig. 8 shows the ergodic capacity gains that we get while moving from non SIC case to SIC case (with no power control) and finally to MU-MIMO scenario. MU-MIMO achieves more capacity gain compared to the other two because of spatial-optical multiplexing of the data stream. The spatial-optical multiplexing is done by carrying different radio signals across different CANs by different optical wavelength. At the HCC the same optical wavelengths are combined in optical domain to get superimposed messages from different MTs with different channel gains.

Fig. 9 shows how the packet transmission time varies for the different schemes with respect to the transmission power

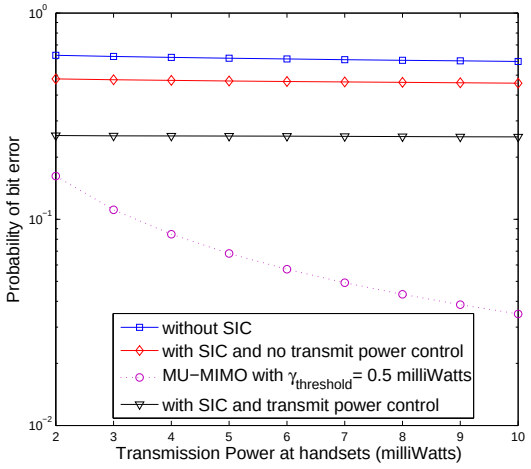

Fig. 10: Probability of Bit error vs. the Transmission power at the MTs.

at the MTs for different packet size. Finally in Fig. 10 the probability of error is plotted against the transmission power at the MTs. The interesting fact is that the first two schemes of without SIC and with SIC does not vary much with increase in transmission power at the MTs. However, the MU-MIMO scheme varies greatly with the variation in transmission power at the MTs which again can be attributed due to the spatial-optical multiplexing of the messages. The parameter of $\gamma_{threshold}$ is set such that the signal power threshold is greater than or equal to 0.5 milli-Watts for individual messages to be assumed decoded. Thus the analysis and simulations help us in establishing that by using our proposed MU-MIMO technique discussed in this paper, we can get a much better performance for such a Fi-Wi uplink channel. Further, we alleviated the problem of hidden nodes in WiFi.

VII. Conclusion

In this paper we proposed a MU-MIMO uplink scheme in the Fi-Wi indoor environment. We discussed about the physical layer aspects of implementing SIC receivers which served as a comparative benchmark for our MU-MIMO scheme. Radio over fiber helps in carrying high data rate to the MTs and thus quenching the ever increasing thirst for higher rates. Increased data rate by joint decoding has been discussed. We resolved the problem of hidden nodes caused due to the CSMA/CA contention mechanism at the MAC layer for WiFi. In this paper we made an attempt to study the WiFi uplink in the Fi-Wi system. We presented a physical layer comparative study of the different transmission schemes. Apart from this, we have found a transmit power control scheme for two MT problem with SIC such that the maximum capacity gain is achieved. The solution for the general case of n MTs follows on the similar lines. Our main contribution in this paper is the schematic and analysis of spatial-optical MU-MIMO uplink scenario. Our paper provides component descriptions that illustrate how such a system can be built in reality. We plan to conduct field trial as our future work, with realistic Fi-Wi channel and take real life measurements. Equally interesting is the study of such a MU-MIMO down-link technique. Different pre-coding and optical wavelength routing mechanisms can be used to mitigate interference between multiple users and also between the multiple streams of a single user served by such a DAS. These are a few potential benefits that arise from having such a hybrid Fi-Wi network. For our future work we are also investigating the potential benefits of such a down-link MU-MIMO Hybrid Fi-Wi networks indoor.

Acknowledgment

The work in this paper is supported by Dutch IOP GenCom MEANS project.

References

[1] A. Kim, Y. H. Joo, and Y. Kim, "60 GHz wireless communication systems with radio-over-fiber links for indoor wireless LANs," *IEEE Transactions on Consumer Electronics*, vol. 50, no. 2, pp. 517 – 520, may 2004.

[2] A. Seeds and T. Ismail, "Broadband access using wireless over multi-mode fiber systems," *Journal of Lightwave Technology*, vol. 28, no. 16, pp. 2430 –2435, aug.15, 2010.

[3] M. Crisp, R. Penty, I. White, and A. Bell, "Wideband radio over fiber distributed antenna systems for energy efficient in-building wireless communications," in *Vehicular Technology Conference (VTC 2010-Spring), 2010 IEEE 71st*, may 2010, pp. 1 –5.

[4] J. Lee and I. Yeom, "Avoiding collision with hidden nodes in IEEE 802.11 wireless networks," *IEEE Communications Letters*, vol. 13, no. 10, pp. 743 –745, october 2009.

[5] L. B. Jiang and S. C. Liew, "Improving throughput and fairness by reducing exposed and hidden nodes in 802.11 networks," *IEEE Transactions on Mobile Computing*, vol. 7, no. 1, pp. 34 –49, jan. 2008.

[6] K. Xu, M. Gerla, and S. Bae, "How effective is the IEEE 802.11 RTS/CTS handshake in ad hoc networks," in *IEEE Global Telecommunications Conference, 2002. GLOBECOM '02.*, vol. 1, nov. 2002, pp. 72 – 76 vol.1.

[7] S.-T. Sheu, T. Chen, J. Chen, and F. Ye, "The impact of rts threshold on IEEE 802.11 MAC protocol," in *Parallel and Distributed Systems, 2002. Proceedings. Ninth International Conference on*, dec. 2002, pp. 267 –272.

[8] J. Kazemitabar and H. Jafarkhani, "Multiuser interference cancellation and detection for users with more than two transmit antennas," *IEEE Transactions on Communications*, vol. 56, no. 4, pp. 574 –583, april 2008.

[9] H. Jin, B. C. Jung, H. Y. Hwang, and D. K. Sung, "A MIMO-based collision mitigation scheme in uplink WLANs," *IEEE Communications Letters*, vol. 12, no. 6, pp. 417 –419, june 2008.

[10] H. Jin, B. C. Jung, and D. K. Sung, "A tradeoff between single-user and multi-user MIMO schemes in multi-rate uplink WLANs," *IEEE Transactions on Wireless Communications*, vol. 10, no. 10, pp. 3332 –3342, october 2011.

[11] H. Jin, J. Cha, and D. K. Sung, "A downlink and uplink collision mitigation scheme for multi-user MIMO-based WLANs through relaying," in *6th International ICST Conference on Communications and Networking in China (CHINACOM), 2011*, aug. 2011, pp. 516 –520.

[12] D. Halperin, T. Anderson, and D. Wetherall, "Taking the sting out of carrier sense: Interference cancellation for Wireless LANs," in *In Proceedings of the 14th ACM international conference on Mobile computing and networking*, 2008.

[13] S. Sen, N. Santhapuri, R. R. Choudhury, and S. Nelakuditi, "Successive interference cancellation: A back-of-the-envelope perspective," in *Proceedings of the 9th ACM SIGCOMM Workshop on Hot Topics in Networks*, ser. Hotnets-IX. New York, NY, USA: ACM, 2010, pp. 17:1–17:6. [Online]. Available: http://doi.acm.org/10.1145/1868447.1868464

[14] D. Tse and P. Viswanath, "Fundamentals of wireless communications," Cambridge, UK, 2004.

[15] P. Mahasukhon, M. Hempel, H. Sharif, T. Zhou, S. Ci, and H.-H. Chen, "BER analysis of 802.11b networks under mobility," in *IEEE International Conference on Communications. ICC '07. 2007*, june 2007, pp. 4722 –4727.

[16] K.-W. Lee, M. Cheng, and L. F. Chang, "Wireless QoS analysis for a Rayleigh fading channel," in *IEEE International Conference on Communications. ICC 98. 1998.*, vol. 2, jun 1998, pp. 1089 –1093 vol.2.